

Assessment and parameterisation of Coulomb-enhanced Auger recombination coefficients in lowly injected crystalline silicon

Pietro P. Altermatt^{a)}

Photovoltaics Special Research Centre, University of New South Wales, Sydney 2052, Australia

Jan Schmidt

Institut für Solarenergieforschung Hameln-Emmerthal (ISFH), 31860 Emmerthal, Germany

Gernot Heiser

School of Computer Science and Engineering, and Photovoltaics Special Research Centre, University of New South Wales, Sydney 2052, Australia

Armin G. Aberle

Institut für Solarenergieforschung Hameln-Emmerthal (ISFH), 31860 Emmerthal, Germany

(Received 10 June 1997; accepted for publication 11 August 1997)

In traditional band-to-band Auger recombination theory, the low-injection carrier lifetime is an inverse quadratic function of the doping density. However, for doping densities below about $3 \times 10^{18} \text{ cm}^{-3}$, the low-injection Auger lifetimes measured in the past on silicon were significantly smaller than predicted by this theory. Recently, a new theory has been developed [A. Hangleiter and R. Häcker, Phys. Rev. Lett. **65**, 215 (1990)] that attributes these deviations to Coulombic interactions between mobile charge carriers. This theory has been supported experimentally to a high degree of accuracy in n-type silicon; however, no satisfactory support for it has been found in p-type silicon for doping densities below $3 \times 10^{17} \text{ cm}^{-3}$. In this work, we investigate the most recent lifetime measurements of crystalline silicon and support experimentally the Coulomb-enhanced Auger theory in p-type silicon in the doping range down to $1 \times 10^{16} \text{ cm}^{-3}$. Based on the experimental data, we present an empirical parameterisation of the low-injection Auger lifetime. This parameterisation is valid in n- and p-type silicon with arbitrary doping concentrations and for temperatures between 70 and 400 K. We implement this parameterisation into a numerical device simulator to demonstrate how the new Auger limit influences the open-circuit voltage capability of silicon solar cells. Further, we briefly discuss why the Auger recombination rates are less enhanced under high-injection conditions than under low-injection conditions. © 1997 American Institute of Physics. [S0021-8979(97)06422-0]

I. INTRODUCTION

In the band-to-band Auger recombination process, an electron recombines with a hole, transferring its excess energy and momentum to another electron or hole. This process is an intrinsic property of silicon because no crystal dislocations or impurity atoms are involved. Such Auger processes are traditionally quantified assuming non-interacting free particles.¹ If the recombining electron-hole pair transfers its energy and momentum to another electron or hole, the process is labelled *eeh* or *ehh*, respectively, and the corresponding recombination rates R are given as¹ $R_{eeh} = C_n n^2 p$ and $R_{ehh} = C_p n p^2$. n and p denote the free electron and hole concentrations. C_n and C_p are the Auger coefficients, which are insensitive to both the dopant type and the dopant concentration in the case of non-interacting free particles.²

The total Auger recombination rate R is the sum of R_{eeh} and R_{ehh} :

$$R = C_n n^2 p + C_p n p^2. \quad (1)$$

The most direct way to determine C_n and C_p experimentally is to measure the carrier recombination lifetime under low-injection conditions in the bulk of a silicon sample as a func-

tion of doping concentration, N_{dop} . This is because under low-injection conditions, i.e., when the excess carrier concentration is much smaller than the majority carrier density, the *eeh* (*ehh*) process dominates in n-type (p-type) silicon. In this case, the low-injection Auger lifetime, τ_A , in n-type material is given by

$$\tau_A = \frac{p - p_o}{C_n n^2 p + C_p n p^2} \approx \frac{p}{C_n n^2 p} = \frac{1}{C_n N_{dop}^2}. \quad (2)$$

An analogous relation holds for p-type material:

$$\tau_A = \frac{1}{C_p N_{dop}^2}. \quad (3)$$

Hence, the corresponding Auger coefficient is obtained from a linear fit of the log-log plot of τ_A vs N_{dop} . The values for the low-injection Auger coefficients that are most often cited in the relevant literature are those determined by Dziewior and Schmid.³ These values are listed in Table I, together with data published by several other authors.⁴⁻⁷ To our knowledge, the recombination lifetimes of Dziewior and Schmid show the smallest scatter of all the lifetime data that were published in the context of low-injection Auger coefficients in silicon. Most of the published Auger

^{a)}Electronic mail: pietro@cse.unsw.edu.au

TABLE I. Published low-injection Auger coefficients C_n and C_p of crystalline silicon at 300 K. Listed are the authors, their published values of C_n and C_p , the range of doping concentration where C_n and C_p were determined, and the measuring techniques applied.

Authors	Coefficients ($\text{cm}^6 \text{s}^{-1}$)	Doping range (cm^{-3})	Measurement technique
Dziewior and Schmid ^a	$C_n = 2.8 \times 10^{-31}$ $C_p = 0.99 \times 10^{-31}$	$6 \times 10^{18} - 1 \times 10^{20}$ $5 \times 10^{18} - 1 \times 10^{20}$	photoluminescence
Beck and Conradt ^b	$C_n = 1.7 \times 10^{-31}$ $C_p = 1.2 \times 10^{-31}$	$2 \times 10^{18} - 2 \times 10^{19}$ $2 \times 10^{18} - 3 \times 10^{19}$	photoluminescence
del Alamo <i>et al.</i> ^c	$C_n = 1.80 \times 10^{-31}$	$6 \times 10^{18} - 6 \times 10^{19}$	photoluminescence
Wang and Neugroschel ^d	$C_n = 2.22 \times 10^{-31}$	$2.5 \times 10^{19} - 8 \times 10^{19}$	transient photocurrent
Wieder ^e	$C_n = 1.6 \times 10^{-31}$	$5 \times 10^{18} - 2 \times 10^{20}$	diffusion length in lateral transistors

^aSee Ref. 3.

^bSee Ref. 4.

^cSee Ref. 5.

^dSee Ref. 6.

^eSee Ref. 7.

coefficients^{4–18} are less reliable than those of Dziewior and Schmid, because they were obtained by less direct measurement techniques.¹

Within the accuracy of the measured lifetime data, C_n and C_p proved to be constant at dopant concentrations above approximately $5 \times 10^{18} \text{ cm}^{-3}$. For lower doping levels, however, smaller lifetimes have been measured than were predicted by the insertion of Dziewior and Schmid's Auger coefficients into Equations (2) and (3). Possible explanations include Shockley-Read-Hall (SRH) recombination^{19,20} via deep defect levels²¹ and via shallow dopants,²² effects of the equilibrium carrier concentration on the injection level,²³ electron-hole plasma interactions,^{24,25} influences of the band occupation statistics,²⁶ as well as trap-assisted,^{8,27} phonon-assisted,²⁸ and Coulomb-enhanced^{29,30} Auger recombination.

To our knowledge, this experimentally observed departure is most generally and precisely quantified by the theory of Hangleiter and Häcker for Coulomb-enhanced Auger recombination.^{29,30} In contrast to the free-particle approximation outlined above, the mobile carriers interact with each other by means of Coulombic interaction. Thus, the electron density is increased in the vicinity of a hole, while it is decreased in the vicinity of another electron. Since the Auger recombination rate strongly depends on the particle densities, recombination is increased by the non-uniform distribution of the charge carriers.³¹ To account for these effects, the Auger coefficients in Equations (2) and (3) are multiplied by the *enhancement factors* g_{eeh} and g_{ehh} , respectively.²⁹ In the quantum mechanical approach of Hangleiter and Häcker, the Coulombic interaction leads to a spatial correlation of electron-hole (e-h) pairs, forming both scattering states and bound states (the latter are called excitons).²⁹ If the majority carriers have a density exceeding the excitonic Mott density of approximately $1 \times 10^{18} \text{ cm}^{-3}$ at 300 K,³² they screen the e-h pair interaction strongly, thus preventing the formation of excitons. As a result, only the scattering states remain, the enhancement factors start to drop towards 1, and the free-particle approximation precisely predicts the Auger rates. It must be emphasised that Hangleiter and Häcker calculated these enhancement factors by means of a quantum statistical

theory without any free parameters.²⁹ They found a reasonable agreement between theory and experiment on n-type silicon. On p-type silicon, however, below a carrier concentration of $3 \times 10^{17} \text{ cm}^{-3}$, their measured lifetimes were significantly lower than those predicted by their theory. This deviation has been attributed to relatively high defect densities in the p-type material investigated.³⁰

In this article we investigate low-injection recombination lifetime data that have been measured very recently.³³ This allows us to extend the doping range where Coulomb-enhanced Auger recombination theory is supported experimentally down to $1 \times 10^{16} \text{ cm}^{-3}$ in p-type silicon. We also compare the new recombination lifetime data with previous results. From a thorough analysis of the collected data we derive new upper limits of the low-injection recombination lifetime in silicon at room temperature. We also suggest an empirical parameterisation of g_{eeh} and g_{ehh} which is useful for numerical simulations of silicon devices at temperatures between 70 and 400 K. We explain how the new low-injection Auger limit influences the open-circuit voltage of silicon solar cells, and why the Auger recombination rates are less enhanced under high-injection conditions than under low-injection conditions.

II. CARRIER LIFETIME MEASUREMENTS

Recently, Schmidt and Aberle³³ developed a novel method for measuring the low-injection carrier recombination lifetime in the bulk of silicon wafers with a high degree of accuracy. In this method, both wafer surfaces are very effectively passivated by remote-plasma silicon nitride films. The circles in Fig. 1 show their measured low-injection carrier recombination lifetime, τ_b , in the bulk of commercially available float-zone (FZ) p-Si wafers with various boron doping densities. The bulk lifetimes were calculated from the measured effective lifetimes using an effective surface recombination velocity, S , of 5 cm/s.³³ Also included in Fig. 1 (lower values of the error bars) are the measured effective lifetimes which, for apparent reasons, represent the lower bounds of the corresponding bulk lifetimes. Figure 1 does

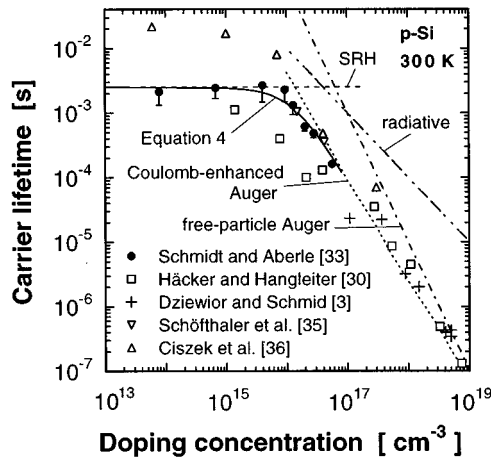


FIG. 1. Measured values of the low-injection carrier recombination lifetime in the bulk of boron-doped silicon at 300 K (symbols), compared to the Coulomb-enhanced (dotted line), to the traditional free-particle (dashed-dotted line) Auger theory, and to radiative recombination. The solid line is calculated using Equation (4) and represents the influence of Shockley-Read-Hall, Coulomb-enhanced Auger and radiative recombination on the measured lifetime values.

not contain upper bounds since, in principle, the recombination could occur completely at the wafer surfaces (i.e., $\tau_b \rightarrow \infty$).

Below the dopant concentration of $1 \times 10^{16} \text{ cm}^{-3}$, an essentially constant lifetime of approximately 2.5 ms has been measured and attributed to SRH recombination. Above that dopant level, the measured lifetime decreases drastically and approaches the theoretical predictions of Hangleiter and Häcker (dotted line).²⁹ Consequently, with increasing doping levels, the dominant recombination mechanism changes from SRH to Auger. The measured τ_b values do not fully reach the dotted line because they are still influenced by SRH recombination. In order to demonstrate this, we calculate τ_b using

$$\frac{1}{\tau_b} = \frac{1}{\tau_{SRH}} + \frac{1}{\tau_{CA}} + \frac{1}{\tau_r}, \quad (4)$$

where $\tau_{SRH} = 2.5 \text{ ms}$ (horizontal dashed line) is the SRH lifetime, τ_{CA} the Coulomb-enhanced Auger lifetime predicted by Hangleiter and Häcker, and τ_r the radiative recombination lifetime.³⁴ The resulting τ_b curve (solid line) correlates closely with the experimental data. Thus, as indicated in Ref. 33, we conclude that the lifetime values are only influenced by $\tau_{SRH} = 2.5 \text{ ms}$, τ_r and τ_{CA} and therefore, as will be discussed below, the theoretical predictions of Hangleiter and Häcker (dotted line) are experimentally supported for lowly injected p-type silicon in the doping range $(1-6) \times 10^{16} \text{ cm}^{-3}$.

An important feature of the data of Ref. 33 is that it scatters very little. This is in contrast to the strongly deviating lifetime values measured by Häcker and Hangleiter³⁰ (squares) and many other authors,^{8-11,17,26} whose data are not shown in Fig. 1. Also included in Fig. 1 are the high-precision measurements of Schöffthaler *et al.*³⁵ and Cizek *et al.*³⁶ on p-type FZ silicon. These data correlate well with

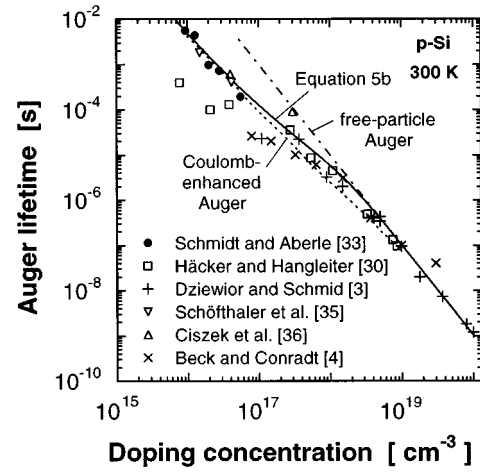


FIG. 2. Auger recombination lifetimes in boron-doped p-type silicon at 300 K, measured under low-injection conditions by various authors (symbols), compared to the Coulomb-enhanced theory of Hangleiter and Häcker (dotted line) and the traditional free-particle Auger theory (dashed-dotted line). The solid line is an empirical fit of the measured maximum lifetime values (Equations (5a) and (5b)), and represents the Auger limit.

the results of Schmidt and Aberle for doping levels above $1.4 \times 10^{16} \text{ cm}^{-3}$. The silicon used by Cizek *et al.* exhibits a very high τ_{SRH} of 21 ms.

III. DISCUSSION

A. New Auger lifetime limit

Figure 2 shows the low-injection Auger lifetimes τ_A measured by various authors in boron-doped silicon at 300 K. The influence of τ_{SRH} and τ_r on the lifetime values is eliminated by Equation (4), using $\tau_{SRH} = 2.5 \text{ ms}$ for the data of Schmidt and Aberle³³ and Schöffthaler *et al.*³⁵ and $\tau_{SRH} = 21 \text{ ms}$ for the data of Cizek *et al.*³⁶ It can be seen from Fig. 2 that the measured τ_A values form a smooth upper lifetime limit (except one data point of Cizek *et al.* at $N_{dop} = 3 \times 10^{17} \text{ cm}^{-3}$), although the silicon material used by the various authors was fabricated under different conditions. If these maximum lifetime values were strongly influenced by extrinsic recombination processes, they would scatter significantly, because the different fabrication conditions of the silicon material would induce a random number of deep defect levels. Thus, we conclude that these maximum values of τ_A are indeed band-to-band Auger limited, and would stay below the solid lines in Figs. 2 and 3 if silicon samples of higher quality had been available in the experiments.

The measured Auger lifetimes deviate significantly from the predictions of Takeshima, whose theory is restricted to Coulombic interactions between scattering states.^{24,25} It is, however, the bound states (excitons) that influence the Auger recombination rate significantly. Therefore, as can be seen from Fig. 2, the measured Auger lifetimes correlate very well with Hangleiter and Häcker's theory for doping levels in the range $1 \times 10^{16} - 1 \times 10^{17} \text{ cm}^{-3}$ and above 10^{19} cm^{-3} (where it approaches the standard theory). However, the measured Auger lifetimes deviate from the predictions of Hangleiter and Häcker in the intermediate doping range ($10^{17} - 10^{19} \text{ cm}^{-3}$).

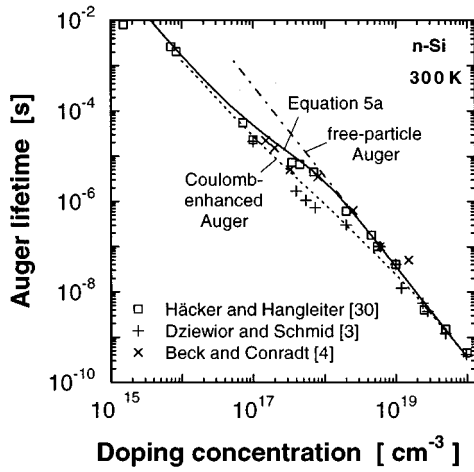


FIG. 3. Same as in Fig. 2, but for phosphorus-doped n-type silicon at 300 K.

Thus, the question arises as to whether the hump in our proposed Auger limit (solid line), located at intermediate doping levels, is an artifact, or whether the theory of Hangleiter and Häcker is too approximate in this doping range. This theory predicts²⁹ such a hump only for low temperatures (70 K), where it has been experimentally confirmed³⁰ in n-type silicon to a high degree of accuracy. In this theory, however, a simple screening model is used that is unable to produce such a hump at room temperature, where the Coulombic correlations are much weaker.³⁷ Thus, we trust the measured maximum lifetime values depicted in Fig. 2, and conclude that such a hump exists even at room temperature, although the reason for this is still under discussion.³⁸ Analogous arguments can be applied to the interpretation of the measured Auger lifetimes in n-type silicon (Fig. 3).

B. Empirical parameterisation for the low-injection Auger coefficients

The solid lines in Figs. 2 and 3 are an empirical fit of the maximum Auger lifetimes, measured in crystalline silicon at 300 K, and represent the low-injection Auger limit. These lines are obtained by replacing the constants C_n and C_p in Equations (2) and (3) with the functions $C_n g_{eeh}$ and $C_p g_{ehh}$, respectively, and using the following expressions for g_{eeh} and g_{ehh} :

$$g_{eeh} = 1 + (g_{max,n} - 1) \times \left(1 - \tanh \left[\left\{ \frac{n}{5 \times 10^{16} \text{ cm}^{-3}} \right\}^{0.347} \right] \right), \quad (5a)$$

$$g_{ehh} = 1 + (g_{max,p} - 1) \times \left(1 - \tanh \left[\left\{ \frac{p}{5 \times 10^{16} \text{ cm}^{-3}} \right\}^{0.297} \right] \right), \quad (5b)$$

with

$$g_{max,n} = 235548 \cdot T^{-1.5013}, \quad g_{max,p} = 564812 \cdot T^{-1.6546}. \quad (5c)$$

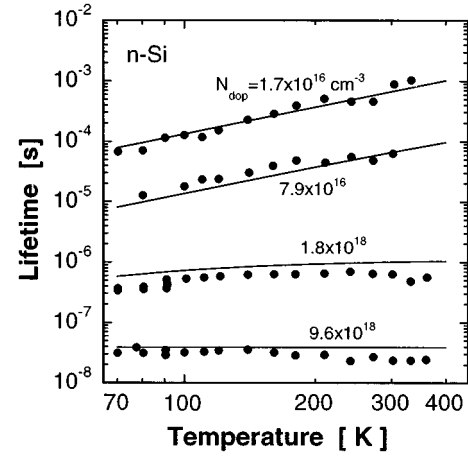


FIG. 4. The parameterisation of the low-injection Auger lifetime as a function of temperature, given by Equation (5a) (solid line), for various phosphorus doping concentrations, compared to experimental lifetime data (see Ref. 39) (symbols).

C_n and C_p are the coefficients of Dziewior and Schmid³ (C_p depends on temperature, and a parameterisation will be given in Equation (6)). The temperature dependence of the enhancement factors results mostly from the properties of the excitons. With decreasing temperature, the excitons are less disturbed by thermal agitation. Therefore, the enhancement factors increase with decreasing temperature, and the doping level at which they drop towards 1 increases as well. Our parameterisation of the Auger lifetime, given by Equations (5a) and (5c), is shown in Fig. 4 (solid lines) as a function of temperature and for various phosphorus doping levels. It correlates well with experimental values (circles).³⁹ These values are, according to Equation (4), influenced by SRH recombination. However, their temperature dependence is ruled by excitonic effects as well, as was investigated in Refs. 40 and 41, and therefore is similar to the temperature dependence of band-to-band Auger recombination.

Figures 5 and 6 show our parameterisation of the Auger lifetime (Equations (5a), (5b), (5c), and (6)) as a function of doping concentration and for various temperatures. Experimental lifetimes, obtained at low temperatures (70 and 77 K), are shown as well. In p-type material, we are lacking experimental data for τ_A at low doping densities and low temperatures. As the theory of Hangleiter and Häcker predicts the experimental lifetimes very precisely at low doping densities and low temperature in n-type silicon,³⁰ we adjust our parameterisation in p-type material to their theory in this temperature and doping range. τ_r at 77 K is obtained from an experimental value, given by Ref. 34 at a doping density of $1 \times 10^{16} \text{ cm}^{-3}$, and is calculated at the other doping densities with Coulomb enhancement considered.³⁹ Calculations⁴² and experiments^{34,42} show that Coulombic interactions cause the radiative recombination rate at such low temperatures to deviate from a linear dependence on n and p .

Within the accuracy of the measurements, C_n is found to be only very weakly dependent on temperature between 70 and 400 K.³ This can be precisely reproduced in this whole temperature range by calculations using only the energy-

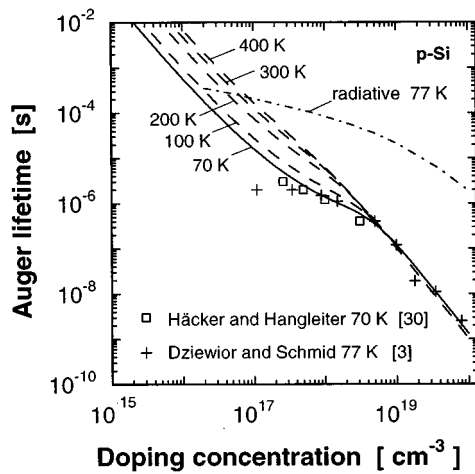


FIG. 5. The parameterisation of the low-injection Auger lifetime in p-type silicon as a function of doping concentration, given by Equations (5b) and (6) (lines), compared to experimental values (symbols) at 70 (see Ref. 30), and 77 K (see Ref. 3). The radiative recombination lifetime (dash-dotted line) is obtained from an experimental value (see Ref. 34) at a doping density of $1 \times 10^{16} \text{ cm}^{-3}$ at 77 K, and is calculated at the other doping densities with Coulomb enhancement considered (see Ref. 39).

momentum relation of silicon.^{2,43} C_p , however, depends on temperature³ and can only be calculated accurately by including phonons that facilitate the momentum match of the carriers involved.⁴⁴ Such processes are called *phonon-assisted* Auger transitions. For the empirical parameterisation of C_p we suggest

$$C_p = 7.91 \times 10^{-32} - 4.13 \times 10^{-35} \cdot T + 3.59 \times 10^{-37} \cdot T^2. \quad (6)$$

This empirical parameterisation is shown in Fig. 7 (solid line) and fits the three experimental data points of Dziewior and Schmid (crosses).³ These authors obtained these data points by a linear fit in the log-log plot of the lifetime vs N_{dop} , as mentioned in Sec. I. In order to show the behavior of C_p between these three data points, we also plot values (circles) that we calculated using Equation (3) from lifetime measurements³⁹ of a *single* sample (with a boron doping

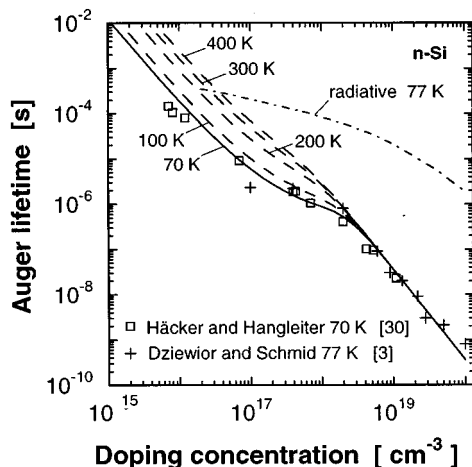


FIG. 6. Same as in Fig. 5, but for phosphorus-doped n-type silicon.

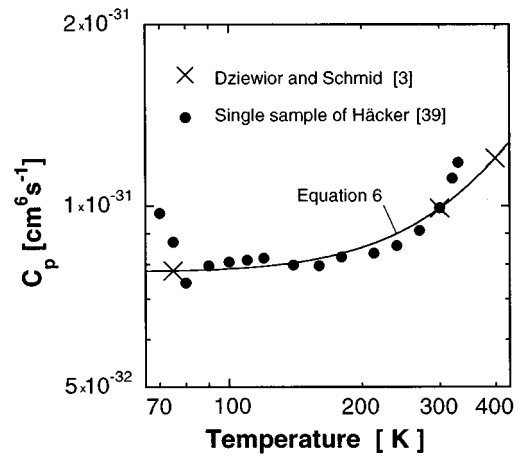


FIG. 7. The parameterisation of C_p as a function of temperature, given by Equation (6) (solid line). It fits the three experimental data points of Dziewior and Schmid (see Ref. 3) (crosses). Also shown are data points, calculated using Equation (3) from lifetime measurements (see Ref. 39) of a single sample (dots).

concentration of $8.5 \times 10^{18} \text{ cm}^{-3}$). For demonstration purposes, we shifted all the circles slightly upwards within the accuracy limits of the measurement technique in order to match them perfectly at 300 K with the values of Dziewior and Schmid. The behavior of C_p is explained as follows.² Below $T \cong 110 \text{ K}$, only the emission of phonons is involved in the Auger process, causing C_p to be independent of temperature. At higher temperatures, an increasing number of phonons is available for absorption during the Auger process, causing C_p to rise.

Our parameterisations (Equations (5a), (5b), (5c) and (6)) are valid only under low-injection conditions and at temperatures between 70 and 400 K. At temperatures below 60 K, the lifetimes increase due to the thermal freeze-out of the majority carriers.⁴⁵ As our parameterisation is simple and continuous, it is suitable for usage in numerical simulations of silicon devices.

C. Auger recombination under high-injection conditions

Under high-injection conditions, the excess carrier concentration, Δn , is much larger than the equilibrium majority carrier concentration. According to the theory of Hangleiter and Häcker, the Auger recombination rate (i.e., g_{eeh} and g_{ehh}) is less enhanced under high-injection conditions than under low-injection conditions if the excess carrier concentration is lower than approximately $5 \times 10^{18} \text{ cm}^{-3}$ at 300 K. The reason for this is that under high injection the densities of free electrons and holes are equal, leading to stronger screening of the Coulombic forces, and thus, compared to heavy doping, to a reduction of the exciton density.²⁹ However, determination of the Auger lifetime is more complicated under high-injection than under low-injection conditions since both *eeh* and *ehh* processes determine the Auger lifetime. Furthermore, the high-injection Auger lifetime, τ_{Ah} , depends on the excess carrier concentration. This can be seen from Equation (1), using $\Delta n = \Delta p$ and $\Delta n \gg n, p$:

$$\tau_{Ah} = \frac{\Delta n}{(C_n + C_p)(\Delta n)^3} \equiv \frac{1}{C_a(\Delta n)^2}. \quad (7)$$

C_a is the so-called *ambipolar* Auger coefficient and is the sum of C_n and C_p . The dependence of g_{eeh} and g_{ehh} on the injection level explains why most of the C_a values reported in the literature (for a review see Refs. 1 and 46) as well as the C_a values used in numerical models of silicon solar cells,^{47–49} are larger than $C_n + C_p$ determined under low-injection conditions (see Table I). The reported values for C_a scatter significantly because they were determined under diverse high-injection conditions, and different evaluation methods have been applied to determine the injection level dependent carrier lifetime. At injection levels between low and high injection, neither C_a nor C_n nor C_p can be directly determined using lifetime measurements.²³

D. Example: Impact of the new Auger limit on Si solar cells

The open-circuit voltage V_{oc} , and hence the energy conversion efficiency, of crystalline silicon solar cells is ultimately limited by Auger recombination.^{50–52} Thus, the low-injection Auger limit proposed in this article limits V_{oc} of those silicon cells that are lowly injected under V_{oc} conditions.

V_{oc} depends on the cell thickness and on the wafer doping concentration.⁵⁰ The silicon solar cells presently exhibiting the highest efficiency under terrestrial sunlight (24.0%) are the n^+p PERL cells made at the University of New South Wales, Sydney. They are made on boron-doped, 370 μm thick float-zone wafers with a doping density of $1.4 \times 10^{16} \text{ cm}^{-3}$.⁵³ In the following we show the impact of the various Auger recombination models on the ultimate one-sun open-circuit voltage of 370 μm thick Si solar cells at 300 K by inserting these models into the numerical device simulation program DESSIS.⁵⁴ We use the device parameters given in Ref. 55. However, in order to be as ideal as possible, we (i) assume negligible SRH recombination losses in the bulk and at the non-contacted surfaces of the cell, and (ii) we change the peak doping density and depth of the phosphorus diffused emitter layer at the front surface from $5 \times 10^{18} \text{ cm}^{-3}$ and 1 μm to $1 \times 10^{19} \text{ cm}^{-3}$ and 0.3 μm , respectively, for wafer (i.e., base) doping densities above $5 \times 10^{17} \text{ cm}^{-3}$. For the band gap narrowing in the heavily doped cell regions, the model proposed by del Alamo *et al.* is used.⁵

Curve a in Fig. 8 shows the dependence of V_{oc} on the boron doping concentration of the wafer, if the traditional free-particle Auger theory is assumed, using the Auger coefficients of Dziewior and Schmid.³ The dashed lines are calculated considering band gap narrowing. As discussed above, for doping levels below $3 \times 10^{18} \text{ cm}^{-3}$, this Auger model seriously overestimates the Auger lifetimes (regardless of the injection level), leading to excessively high open-circuit voltages.

Curve b in Fig. 8 shows the calculated V_{oc} if our parameterisation of the low-injection Auger lifetime is used. Obviously, the V_{oc} obtainable is drastically reduced. However, under one-sun illumination, the wafer doping concentration has to be above approximately $5 \times 10^{16} \text{ cm}^{-3}$ in 370 μm

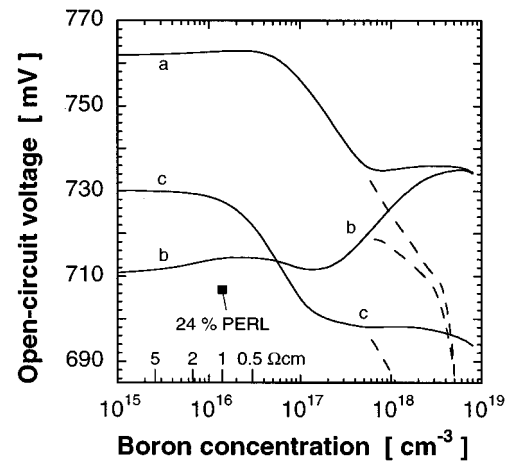


FIG. 8. Ultimate one-sun open-circuit voltage, V_{oc} , simulated for a 370 μm thick n^+p silicon solar cell, as a function of the boron doping density in the base. For the Auger recombination, the free-particle theory [Equation (3) with C_p of Dziewior and Schmid (see Ref. 3)] is used in curve a, our parameterisation for the case of low injection [Equations (5b) and (5c)] in curve b, and the free-particle theory with C_a for high injection (Sinton and Swanson, see Ref. 47) in curve c. The dashed lines are calculated considering band gap narrowing. The fabricated PERL silicon cells with 24% efficiency are shown as squares.

thick cells to ensure low-injection conditions and, therefore, curve b is only valid for $N_{dop} > 5 \times 10^{16} \text{ cm}^{-3}$.

In the case of lightly doped wafers (well below $1 \times 10^{16} \text{ cm}^{-3}$ in 370 μm thick cells), the base of the solar cell is highly injected under one-sun V_{oc} conditions. Therefore, we chose the ambipolar Auger coefficient $C_a = 2.4 \times 10^{-30} \text{ cm}^6 \text{ s}^{-2}$, measured by Sinton and Swanson,⁴⁷ and obtained curve c in Fig. 8. Curve c is only valid for $N_{dop} < 5 \times 10^{15} \text{ cm}^{-3}$.

Considering band gap narrowing (dashed lines), it follows from Fig. 8 that the highest V_{oc} is obtained if the cell operates under high-injection conditions. However, the 24% record-efficiency PERL cells mentioned above operate near V_{oc} at intermediate injection levels (i.e., between low and high injection) because they are fabricated on 370 μm thick wafers with $N_{dop} = 1.4 \times 10^{16} \text{ cm}^{-3}$. In order to determine the actual behavior of 200–400 μm thick cells at doping levels around $1 \times 10^{16} \text{ cm}^{-3}$, new measurements of the Auger lifetime at intermediate injection levels have to be performed.

IV. SUMMARY

In this work, the most recent low-injection carrier recombination lifetime measurements on float-zone crystalline silicon are investigated. In p-type silicon, analysis of the measured data allows us to extend the doping range where the Coulomb-enhanced Auger recombination theory is experimentally supported down to $1 \times 10^{16} \text{ cm}^{-3}$ at 300 K.

Based on the experimental data, a re-assessment of the upper limit of the low-injection carrier lifetime in n- and p-type silicon is made. An empirical parameterisation for the new Auger limit is proposed which describes the dependence

of the low-injection Auger coefficients C_n and C_p on both the doping concentration and the temperature. This parameterisation is suitable for usage in numerical simulations of silicon devices at temperatures between 70 and 400 K. This is demonstrated by simulating the ultimately obtainable open-circuit voltage of a Si solar cell under terrestrial illumination. These simulations show that the V_{oc} limit is higher under high-injection conditions than under low-injection conditions.

ACKNOWLEDGMENTS

One of the authors (P. P. A.) is grateful for fruitful discussions with A. Hangleiter. He also thanks A. Cuevas, M. A. Green, V. Henninger, R. R. King, A. Schenk and R. A. Sinton for valuable discussions. Two of the authors (J. S. and A. G. A.) thank R. Hezel for his continuous support. The ISFH is supported by the federal state of Lower Saxony and the German Bundesministerium für Bildung, Wissenschaft, Forschung und Technologie. The ISFH is a member of the German Forschungsverbund Sonnenenergie. The work of one author (G.H.) was supported by a grant from the Australian Research Council. The Photovoltaics Special Research Center is supported by the Australian Research Council's Special Research Centres Scheme and by Pacific Power.

- ¹M. Tyagi and R. van Overstraeten, *Solid-State Electron.* **26**, 577 (1983).
- ²D. Laks, G. Neumark, and S. Pantelides, *Phys. Rev. B* **42**, 5176 (1990).
- ³J. Dziewior and W. Schmid, *Appl. Phys. Lett.* **31**, 346 (1977).
- ⁴J. Beck and R. Conradt, *Solid State Commun.* **13**, 93 (1973).
- ⁵J. del Alamo, S. Swirhun, and R. M. Swanson, *Tech. Dig. Int. Electron Devices Meet.*, 290 (1985).
- ⁶C. H. Wang and A. Neugroschel, *IEEE Electron Device Lett.* **11**, 576 (1990).
- ⁷A. Wieder, *IEEE Trans. Electron Devices* **27**, 1402 (1980).
- ⁸J. Fossum, R. Mertens, D. Lee, and J. Nijs, *Solid-State Electron.* **26**, 569 (1983).
- ⁹D. Huber, A. Bachmeier, R. Wahlrich, and H. Herzer, *Proceedings of the Fifth International Symposium on Silicon Materials Science and Technology*, Boston, MA 1986, pp. 1022–1032.
- ¹⁰P. A. Iles and S. I. Soclof, *Proceedings of the 11th IEEE Photovoltaic Specialists Conference*, Scottsdale, AZ, 1975, p. 19.
- ¹¹J. Krausse, *Solid-State Electron.* **17**, 427 (1974).
- ¹²G. Krieger and R. Swanson, *J. Appl. Phys.* **54**, 3456 (1983).
- ¹³R. Mertens, J. L. van Meerbergen, J. Nijs, and R. van Overstraeten, *IEEE Trans. Electron Devices* **27**, 949 (1980).
- ¹⁴L. Passari and E. Susi, *J. Appl. Phys.* **54**, 3935 (1983).
- ¹⁵G. Possin, M. Adler, and B. Baliga, *IEEE Trans. Electron Devices* **27**, 983 (1980).
- ¹⁶D. Roulson, N. Arora, and S. Chamberlain, *IEEE Trans. Electron Devices* **29**, 284 (1982).
- ¹⁷W. W. Seng, *IEEE Trans. Electron Devices* **22**, 25 (1975).
- ¹⁸H. Weaver and R. Nasby, *IEEE Trans. Electron Devices* **28**, 465 (1981).
- ¹⁹W. Shockley and W. Read, *Phys. Rev.* **87**, 835 (1952).
- ²⁰R. Hall, *Phys. Rev.* **87**, 387 (1952).
- ²¹J. G. Fossum and D. S. Lee, *Solid-State Electron.* **25**, 741 (1982).
- ²²C. Hu and W. Oldham, *Appl. Phys. Lett.* **35**, 636 (1979).
- ²³A. Hang, *J. Phys. C* **21**, L287 (1988).
- ²⁴M. Takeshima, *Phys. Rev.* **26**, 917 (1982).
- ²⁵M. Takeshima, *Phys. Rev.* **28**, 2039 (1983).
- ²⁶Y. Vaitkus and V. Grivitskas, *Sov. Phys. Semicond.* **15**, 1102 (1981).
- ²⁷P. Landsberg, *Solid-State Electron.* **30**, 1107 (1987).
- ²⁸K. Betzler and R. Conradt, *Solid State Commun.* **17**, 823 (1975).
- ²⁹A. Hangleiter and R. Häcker, *Phys. Rev. Lett.* **65**, 215 (1990).
- ³⁰R. Häcker and A. Hangleiter, *J. Appl. Phys.* **75**, 7570 (1994).
- ³¹A. R. Beattie and P. T. Landsberg, *Proc. Phys. Soc. London, Sect. A* **429**, 16 (1958).
- ³²N. F. Mott, *Metal-insulator Transitions* (Taylor and Francis, London, 1974).
- ³³J. Schmidt and A. G. Aberle, *J. Appl. Phys.* **81**, 6186 (1997).
- ³⁴H. Schlängenotto, H. Maeder, and W. Gerlach, *Phys. Status Solidi A* **21**, 357 (1974).
- ³⁵M. Schöfthaler, R. Brendel, G. Langguth, and J. Werner, *1st World Conference on Photovoltaic Energy Conversion*, Waikaloa, HI, 1994, pp. 1509–1513.
- ³⁶T. Cizek, T. Wang, T. Schuyler, and A. Rohatgi, *J. Electrochem. Soc.* **136**, 230 (1989).
- ³⁷A. Hangleiter (private communication, 1996).
- ³⁸M. A. Green and P. P. Altermatt (unpublished).
- ³⁹R. F. Häcker, Ph.D. thesis, University of Stuttgart, Germany, 1991.
- ⁴⁰A. Hangleiter, *Phys. Rev. B* **35**, 9149 (1987).
- ⁴¹A. Hangleiter, *Phys. Rev. B* **37**, 2594 (1988).
- ⁴²A. Hangleiter, *Habilitation thesis*, University of Stuttgart, Germany, 1992.
- ⁴³D. B. Laks, G. F. Neumark, A. Hangleiter, and S. T. Pantelides, *Phys. Rev. Lett.* **61**, 1229 (1988).
- ⁴⁴W. Lochmann and A. Haug, *Solid State Commun.* **35**, 553 (1980).
- ⁴⁵F. J. Morin and J. P. Maita, *Phys. Rev.* **96**, 28 (1954).
- ⁴⁶P. Jonsson, H. Bleichner, and E. Nordlander, *J. Appl. Phys.* **81**, 2256 (1997).
- ⁴⁷R. Sinton and R. Swanson, *IEEE Trans. Electron Devices* **34**, 1380 (1987).
- ⁴⁸P. P. Altermatt, G. Heiser, X. Dai, J. Jürgens, A. G. Aberle, S. J. Robinsons, T. Young, S. R. Wenham, and M. A. Green, *J. Appl. Phys.* **80**, 3574 (1996).
- ⁴⁹P. A. Basore, *Proceedings of the 20th IEEE Photovoltaic Specialists Conference*, Las Vegas, NV, 1988, pp. 389–396.
- ⁵⁰M. A. Green, *IEEE Trans. Electron Devices* **31**, 671 (1984).
- ⁵¹T. Tiedje, E. Yablonovitch, G. Cody, and B. Brooks, *IEEE Trans. Electron Devices* **31**, 711 (1984).
- ⁵²M. A. Green, *Silicon Solar Cells: Advanced Principles and Practice* (Bridge Printery, Sydney, Australia, 1995).
- ⁵³J. Zhao, A. Wang, P. P. Altermatt, S. R. Wenham, and M. A. Green in *Ref. 35*, pp. 1477–1280.
- ⁵⁴DESSIS 3.0: *Manual* (ISE Integrated Systems Engineering AG, Zurich, Switzerland, March 1996).
- ⁵⁵P. P. Altermatt, G. Heiser, A. G. Aberle, A. Wang, J. Zhao, S. J. Robinsons, S. Bowden, and M. A. Green, *Prog. Photovolt.* **4**, 399 (1996).